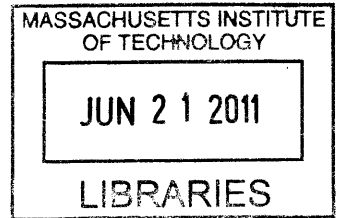


**Electrical Noise Model for Detection Circuitry
of an NMR-Based Formation Evaluation Tool**

By

Julie Laure K. Maison

S.B. EE, M.I.T., 2009



ARCHIVES

Submitted to the Department of Electrical Engineering and Computer Science

in partial fulfillment of the Requirements for the Degree of

Master of Engineering in Electrical Engineering and Computer Science

At the Massachusetts Institute of Technology

January, 2011

[February 2011]

©2011 Massachusetts Institute of Technology
All rights reserved.

The author hereby grants to M.I.T. permission to reproduce and to distribute publicly paper and electronic copies of this thesis document in whole and in part in any medium now known or hereafter created.

Author _____
Department of Electrical Engineering and Computer Science
June 10, 2010

Certified by _____
[Supervisor's Name and Title]
VI-A Company Thesis Supervisor

Certified by _____
Associate Professor EECS, M.I.T. Thesis Supervisor

Accepted by _____
Dr. Christopher J. Terman

Chairman, Department Committee on Graduate Theses

Electrical Noise Model for the Detection Circuitry
of an NMR-Based Formation Evaluation Tool

by
Julie Laure K. Maison

Submitted to the
Department of Electrical Engineering and Computer Science

January 11th, 2011

In partial fulfillment of the Requirements for the Degree of
Master of Engineering in Electrical Engineering and Computer Science

ABSTRACT

The RF signals received from Nuclear Magnetic Resonance (NMR) measurements in logging while drilling NMR instruments are often of the same amplitude as the noise generated by the instruments. Designers of these devices are thus usually faced with the challenging task of improving the sensitivity of the measurement process either by reducing the noise generated by the system or by boosting the signal relative to the electrical noise. For NMR equipment used in earth formation evaluation, this is rendered more difficult by the measurement geometry and noise of the samples under consideration.

Schlumberger's proVISION logging-while-drilling tool is one such NMR device. It makes use of the technique of NMR to evaluate the porosity of the earth's rock formations. Although the tool boosts the signal-to-noise ratio (SNR) to a level sufficient for productivity analysis, SNR improvement is a continuing goal to improve signal quality and provide better results to help optimize the drilling process. The objective of this thesis is to model the electrical noise in the detection path of the NMR signal of the proVISION tool. Intrinsic and extrinsic noise sources contributing to the overall electrical noise in the acquisition path prior to digital processing of the detected signal are accounted for by this model. The results of this analysis provide the necessary data for further SNR improvements in the system.

Thesis Supervisors:

MIT: Elfar Adalsteinsson

Title: Associate Professor of Electrical Engineering & Computer Science, RLE; Associate Professor of Health Sciences and Technology - Magnetic Resonance Imaging Group Director

Schlumberger:

Brian Boling

Title: Project Manager , Schlumberger Houston Formation Evaluation Integration Center
Aurora Kennedy

Title: Senior Electrical Engineer, Schlumberger Houston Formation Evaluation Integration Center

Acknowledgements

The execution of this thesis would not have been possible without the help of several people I am very indebted to. It was a huge honor to have worked with the proVISION Team at the Schlumberger Houston Formation Evaluation Integration Center. They provided a happy and supportive atmosphere that made work really enjoyable. I would especially like to thank my manager, Brian Boling, and supervisor, Aurora Kennedy, for providing me with this project in the first place, for always being present when I needed advice on my work, for making available (or giving me directives to) all the academic and technical assistance I needed, for encouraging me throughout the project, and for keeping me focused whenever I got side-tracked. They are exemplary mentors and engineers that I look up to, and I hope to enjoy my work as much as they do when I graduate.

I am also very grateful to the engineers, scientists and technicians at the same facility who were always available to answer all my questions and who, together with my team, helped me gain a better understanding of my research.

At MIT I am immensely grateful to my thesis advisor Prof. Elfar Adalsteinsson for agreeing to supervise this thesis, for his suggestions and recommendations, for helping me put my academic work in perspective when I was becoming too detailed for my own good, and for helping me find the necessary resources on campus to facilitate my project. I am also hugely indebted to Prof. Peter Hagelstein, my MEng advisor, for his support with all my academic work this year and for always making time for all the forms I had for him. I would also like to thank the Course 6 Undergraduate Office for the relaxing talks whenever I stopped by to check on deadlines and to the department Professors who took time off their hectic schedules to enlighten me on electrical noise, especially Prof. Vladimir Stojanovic and Prof. Joel Dawson.

I am most indebted to the VI-A directors and Julius Kusuma for giving me the opportunity to work with a great company on really interesting projects. Each assignment helped me appreciate the challenges of my field a lot more and made me absolutely love even my hardest classes this semester.

Finally I would like to thank my family for their continuous moral and mocking support, especially as (Doctor!) Michele raced to finish her thesis as well, and my friends for the all-nighters, the wake-up calls and fun they inflicted upon me as I wrote my thesis.

Table of Contents

1. Introduction.....	6
1.1 Electrical Noise Theory	6
1.1.1 Johnson noise	7
1.1.2 Shot Noise.....	7
1.1.3 1/f Noise	8
1.1.4 Interference	8
1.1.5 Quantization Noise	8
1.2 Noise Equivalent Representation	9
1.2.1 Resistors.....	9
1.2.2 Diodes (and all other p-n junctions)	9
1.2.1 Amplifiers.....	10
2.ProVision Overview	11
3.Experimental Methodology 3.1 SPICE simulation	13
3.2 Confirmation Experiments.....	16
3.2.1 Apparatus and Materials	16
3.2.2. List of Tests	17
3.2.3 Experimental Procedure	18
4. Results	19
5. Discussion	33
5.1 Recommendations.....	34
5.2 Conclusion	35
Appendix.....	36
A. Important Definitions.....	36
A.1 Noise Bandwidth, Δf	36
A. 2 Nuclear Magnetic Resonance (NMR)	36
A.3 SPICE.....	37
B. Sample Calculation and Equivalent Simulation	38
C. References.....	41

List of Figures

Figure 1- 1 Noise equivalent resistor circuit.....	9
Figure 1- 2 Noise Equivalent Diode Circuit	9
Figure 1- 3 Noise Equivalent Amplifier Circuit	10
Figure 2- 1 NMR System block diagram	12
Figure 3 - 1 SPICE Noise Modeling of an Amplifier	15
Figure 3 - 2 Detection Circuitry Under Consideration.	18
Figure 4 - 1 Gain as a Function of Frequency at stage I.....	19
Figure 4 - 5 Measured Noise Voltage vs. Frequency at Stage 1 VII.	23
Figure 4 - 6 Simulated Gain at 245KHz for Stages 1 Through 7	24
Figure 4 - 7 Simulated Antenna-Referenced Noise Voltage Input at 245KHz for Stages 1 Through 7.....	25
Figure 4 - 9 Simulated Noise Voltage vs. Temperature at Larmor Frequency.....	27
Figure 4 - 10 Measured Noise Voltage vs. Temperature at Larmor Frequency.	28
Figure 4 - 13 Difference in Measured Noise Voltage vs. Frequency at Stage 7 with Noise Source 1 On vs. Off.....	30
Figure B-1: Noisy circuit as described in SPICE simulation example	38
Fig B-2: Noise Plot of B-1 circuit.....	39

1. Introduction

The proVISION tool is part of a family of Schlumberger tools that uses Nuclear Magnetic Resonance (NMR) to evaluate the earth's rock formations. Nuclear Magnetic Resonance is a phenomenon exhibited by certain atoms in the presence of a static magnetic field and electromagnetic pulse. These atoms absorb energy from the pulse and radiate it back out as a detectable RF signal. The NMR signals generated in the earth's formation and received by the antenna are typically on the order of a few nano-volts and need to be amplified for detection. However, amplification of these signals simultaneously amplifies the electrical noise at the input of the system and the noise generated by activities in the earth's formation, which can also contribute additional noise in the frequency band of interest. This noise obstructs the detection of the RF signal. In the case of the proVISION tool, care has been taken to ensure that the SNR is adequate to meet the needs of the market, but further noise reduction is always a continuing goal to help provide answers to better optimize the drilling process.

1.1 Electrical Noise Theory

Electrical noise generally refers to any unwanted, random disturbances generated by electrical devices that contaminate a signal of interest. Although the instantaneous value of this noise cannot be predicted, its statistical properties can often be modeled by a Gaussian probability density function centered at a zero mean and with standard deviation σ , the RMS value of the noise voltage. In extreme cases, electrical noise can be significant enough to cause component damage and prevent the proper functioning of an electrical system. Knowledge of the different noise sources present in a system is crucial to its modeling, measurement and attenuation.

The most common types of electrical noise inherent to an electrical system are Thermal or Johnson noise, Shot noise and Low-Frequency noise.

1.1.1 Johnson noise

Johnson noise is inherent to all thermally agitated conducting particles and ceases to exist only at absolute zero (0K). It is characterized by a constant spectral density. The noise current contribution of the Johnson noise through a conductor is given by:

$$I_t = \sqrt{\frac{4K_B T \Delta f}{R}}$$

, where K_B = Boltzmann's constant ($1.38 \times 10^{-23} \text{JK}^{-1}$)

T = Absolute temperature

Δf = Noise bandwidth

R = Real part of the conductor's impedance.

From the above equation one could deduce that open circuits would produce infinite Johnson noise. The noise voltage is controlled due to some shunt capacitance. This limiting effect is known as **kT/C noise**.

1.1.2 Shot Noise

Shot noise is associated with variations in subatomic current impulses at potential barriers during direct current flow. Its spectral density is white up to specific frequencies related to transit time of a charged particle through a conductor. Its value at any p-n junction is given by:

$$I_{sh} = \sqrt{2q I_{DC} \Delta f}$$

, where q = Electronic charge ($1.602 \times 10^{-19} \text{C}$)

I_{DC} = Direct current through the junction.

1.1.3 1/f Noise

Low frequency noise is a hybrid of white noise that is uncorrelated in time and Brownian motion noise (integral of white noise) uncorrelated in increments, which increases limitlessly with decreasing frequency, and is hence prevalent at low frequencies.

1.1.4 Interference

RF signals such as those measured by the device under inspection, are almost unavoidably vulnerable to external noise agents, commonly referred to as interference. These agents can be categorized as:

- Unintentional RF interference, most frequently from cables connected to an electrostatic discharge source. These serve as RF-propagating antennas which can interfere with a desired signal.
- Intentional RF interference which includes a huge array of transmitting devices such as commercial radios, remote controls, broadcast transmitters, cellular phones and motion sensors.

1.1.5 Quantization Noise

Quantization noise arises at the level of digital processing of analog signals; it is the difference between the actual analog value and the quantized digital value of a signal. In the case where this difference is uniformly distributed between -1/2 LSB and +1/2 LSB, the Signal-to-Noise Quantization Ratio(SQNR) is given by:

$$\text{SQNR} = 20 \log_{10}(2^Q) \approx 6.02 \cdot Q \text{ dB}, \text{ where } Q = \text{resolution in bits.}$$

1.2 Noise Equivalent Representation

The noise equivalent circuit components based on the above discussion are illustrated below.

1.2.1 Resistors

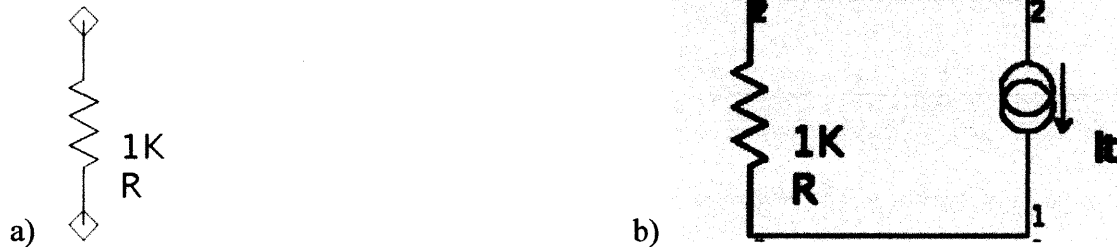


Figure 1- 1 Noise equivalent resistor circuit.

The resistor in figure a) is replaced by the noise-equivalent circuit in figure b) above.

1.2.2 Diodes (and all other p-n junctions)

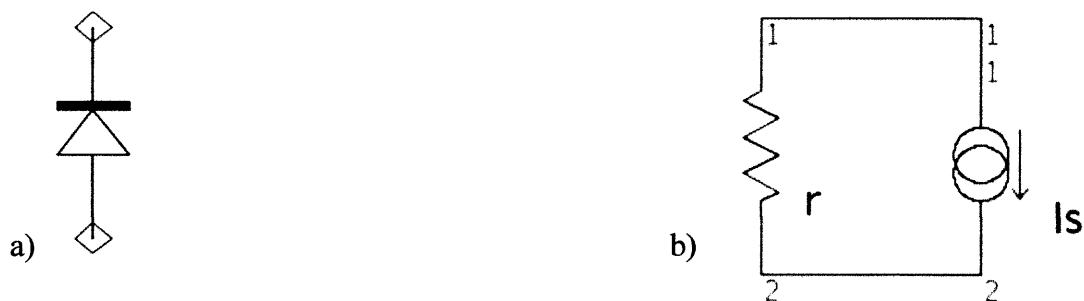
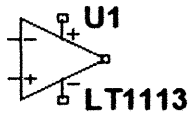


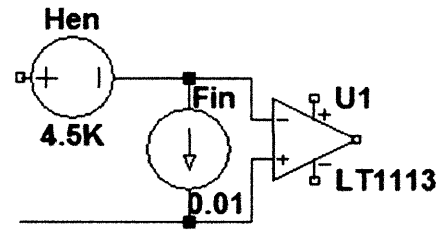
Figure 1- 2 Noise Equivalent Diode Circuit

Diode a) is represented by circuit b) above. I_s is the shot noise of the diode as per 1.1.2 above. R from 1.2.1 is set to $2KT/q \cdot I_E$ so that its equivalent I_t has the same value as the shot noise. This is one way of representing shot noise in a diode.

1.2.1 Amplifiers



a)



b)

Figure 1- 3 Noise Equivalent Amplifier Circuit

Hen and Fin correspond to the voltage and current sources representing the sum of all the noise voltages and currents in the amplifier caused by Johnson and shot noise.

2.ProVision Overview

The proVISION tool uses Nuclear Magnetic Resonance measurements to provide a real-time estimate of the porosity, free fluid index and pore-size distribution of earth formations independent of mineralogy. The tool has provided the oilfield industry with a highly accurate representation of formation productivity since its inception. The general electronic block diagram of an NMR system like proVISION is illustrated in figure 4 below.

The system under analysis is the detection circuitry shown in the dashed area. It consists of a duplexer to allow the transmitter and receiver to share the antenna while keeping them isolated, a preamplifier, a receiver board, and acquisition circuitry that includes analog-to-digital conversion. The electrical noise model created for this detection circuitry would help the group optimize formation evaluation.

Preliminary studies showed that of the three fundamental types of electrical noise, only Johnson and shot noise are relevant in the detection circuitry under analysis, given the frequency range of interest. These noise currents, alongside amplifier noise current and voltages inherent to amplifiers caused by the same noise phenomena, are subject to the same gain and attenuation processes as the signal of interest. The cumulative result competes with the actual NMR signal at the input of the acquisition ADC.

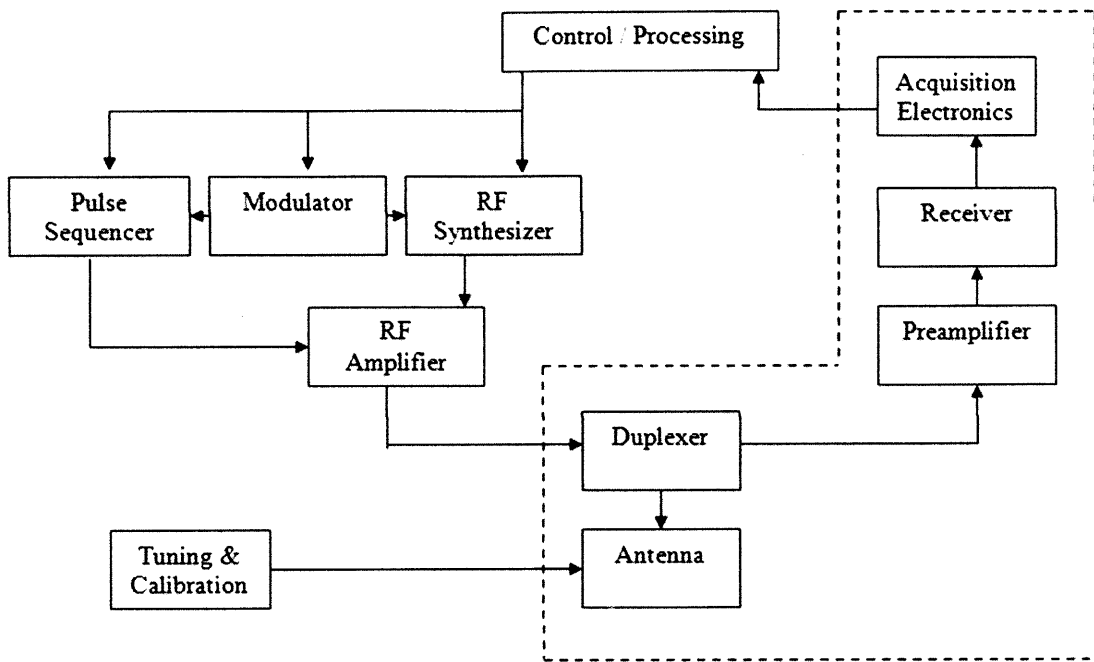


Figure 2- 1 NMR System block diagram

See Appendix A for further explanation.

3. Experimental Methodology

3.1 SPICE simulation

In order to model the electrical noise in circuits, analysts must replace each circuit component by their noise equivalent (see section 1.2 above) and sum up the weighted noise sources to obtain the total noise at a node of interest. This can be done manually but becomes more error-prone and time-consuming with increasing circuit complexity. Consequently for circuits like an NMR acquisition front end, circuit simulation software that is capable of executing these computations like SPICE (University of California, Berkeley) becomes an attractive noise modeling platform.

For this research ICAP/4 SPICE (Intusoft, Carson-California) software was used because of its extensive device library and user-friendly design interface. When ICAP was not available LTSpice was used as it was a cost-effective option. The .NOISE statement in SPICE allows users to perform eponymous noise analysis. SPICE accordingly computes:

- a) The thermal noise in every resistor without explicit addition of their associated noise sources to a netlist.
- b) The shot noise for every diode and transistor.

Hence:

```
.NOISE V(5) VIN 10
```

would instantiate noise analysis at output node 5. The noise at this node would be referred at VIN with a summing interval of 10. The results of this analysis can be displayed in terms of output noise or input noise over a spectrum of interest. Most of the parameters on which the

noise depends like temperature, noise bandwidth and resistance can be altered in the simulator to observe noise variations. The ideal noise model created could thus be compared with the real system to verify simulated noise dependence on temperature, antenna impedance and other factors predicted by the model.

Amplifiers, ADCs and other components of higher complexity than resistors, diodes and transistors must have noise voltages and currents connected as noise sources at the input of the components. This can be done in many ways in SPICE; the method used for this analysis was the use of resistors as noise sources. The noise was reflected to nodes of interest through current-controlled current and noise sources. The exact input noise voltage and current for these ICs are usually available on specification sheets.

Consider, for example, an LT1113 JFET operational amplifier with typical input noise voltage of $4.5\text{nV}/\sqrt{\text{Hz}}$ and its noise current is $10\text{fA}/\sqrt{\text{Hz}}$. To produce a noise current of $1\text{pA}/\sqrt{\text{Hz}}$, we need a resistance, R_{base} such that:

$$R_{\text{base}} = 4kT/1\text{pA} \text{ (see section X)}$$

$$\Rightarrow R_{\text{base}} = 4 * 1.38 * 10^{-23} * 300 / 10^{-24}$$

$$= 16.56\text{K}\Omega$$

Let the op-amps noise current and noise voltage be I_n and E_n respectively. Both sources are usually uncorrelated and would consequently each need a different R_{base} . The noise equivalent circuit of the LT1113 would consequently be:

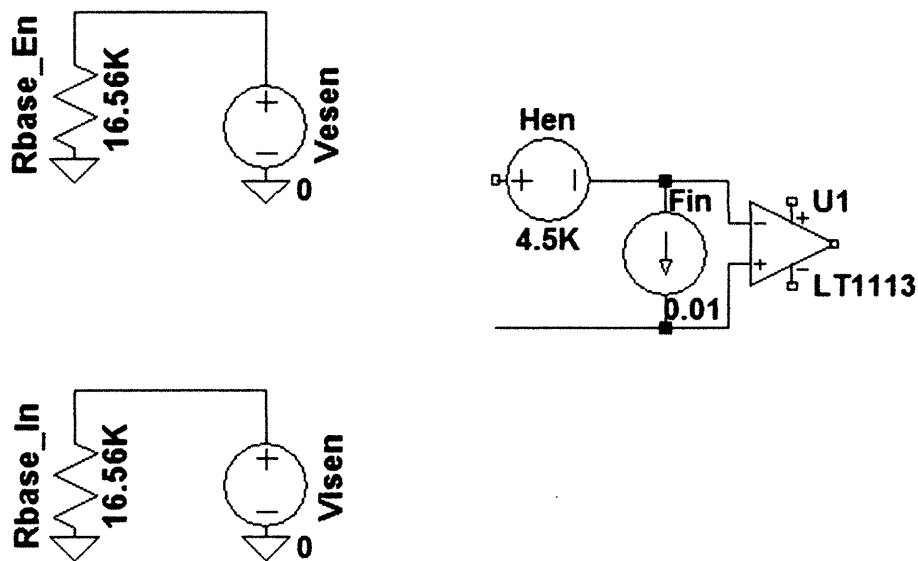


Figure 3 - 1 SPICE Noise Modeling of an Amplifier

(For Netlist see appendix.)

SPICE can thus be used to model the ideal electrical noise in the detector, upon which other sources of electrical disturbance can be added to completely account for the noise in the detection system. The validity of the simulation results can then be verified with manual calculations of the generated noise in smaller sections of the circuit. (See Appendix B). This technique was used on the detection circuitry under analysis which is not illustrated to preserve confidentiality.

A defect of this modeling technique is that it does not consider preceding circuitry that could overshadow the electrical noise level of the system under consideration. The executed simulation did not take into account possible transmitter noise contribution through the shared duplexer.

Another problem researchers carrying out similar experiments could face is the lack of electrical noise current and voltage specifications in some datasheets, or the unsuitability of given values for test conditions differing from those stated, which would require manual tests to obtain these values.

3.2 Confirmation Experiments

Upon completion of the SPICE simulations, the analyzed circuit had to be compared to the real circuits for validation. This investigation was carried out in the lab at Schlumberger's Sugar Land campus under the supervision of the project team. The system noise response to potential external noise agents was also measured.

3.2.1 Apparatus and Materials

The following equipment is indispensable to the successful execution of the project:

- Standard Schlumberger internal network – accessible work station
- proVISION tool
- Power supplies for low and high voltage generation
- A network analyzer
- A spectrum analyzer
- A GPIB-USB-HS for data capture from the spectrum analyzer if older model is used.
- LabVIEW for communication with the spectrum analyzer

- Several BNC cables, splitters and electric probes.
- Personal protective gear (lab coats, hard hats, steel-toed boots and protective goggles)
- Soldering equipment
- An oven

3.2.1.1 Precautions

Standard precautions observed in engineering laboratories are recommended. In addition the following behavior is highly encouraged for experimenters.

- Personal protective gear must be worn at all times in the lab.
- The high voltage power supply should always be turned on last or not at all (for these tests). When shutting down the system it is turned off first.
- Most of the apparatus is heavy and needs to be handled with care.
- Appropriate shielding measures should to be taken in the lab as nearby tools could easily interfere with signals of interest. Running the tests outside of normal work hours is recommended to reduce possible interference from tools in the vicinity of the tool under test.
- The magnet that provides the static B-field is very strong. It could easily affect experimenters' personal items like magnetic stripe cards. It is recommended that these be kept outside the premises of the lab

3.2.2. List of Tests

- Noise vs. frequency
- Noise per stage

- Noise vs. tool temperature
- Noise vs. input impedance
- Acquisition effect on noise
- High voltage effect on noise

3.2.3 Experimental Procedure

- At the initial state of every test the antenna is disconnected from the tool and the input of the duplexer board is grounded.
- The spectrum under consideration for LabVIEW and the instruments used is 200KHz to 300KHz as the system's frequency of operation lies in this range.
- Measurements were made at the stages the system represented by the figure below:

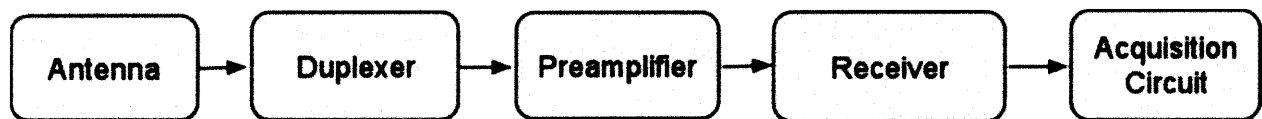


Figure 3 - 2 Detection Circuitry Under Consideration.

Stage I was at the output of the duplexer, stage II at the output of the preamplifier, stages III through VI were test points on the receiver board and Stage VII was a test point on the acquisition board.

4. Results

The simulation noise variations were in the same direction as the gain at each stage of the circuit or at different frequencies in the spectrum. Overall the noise variation across the different stages of the system favored the model. The graphs obtained from the experiments were however less gently varying. The main anomalies that were observed were:

1. Noise spikes at frequencies other than the operation frequency and contrary to the SPICE model.
2. Periodic spikes in noise.
3. A deviation in Noise vs. antenna impedance below a critical impedance, Γ .

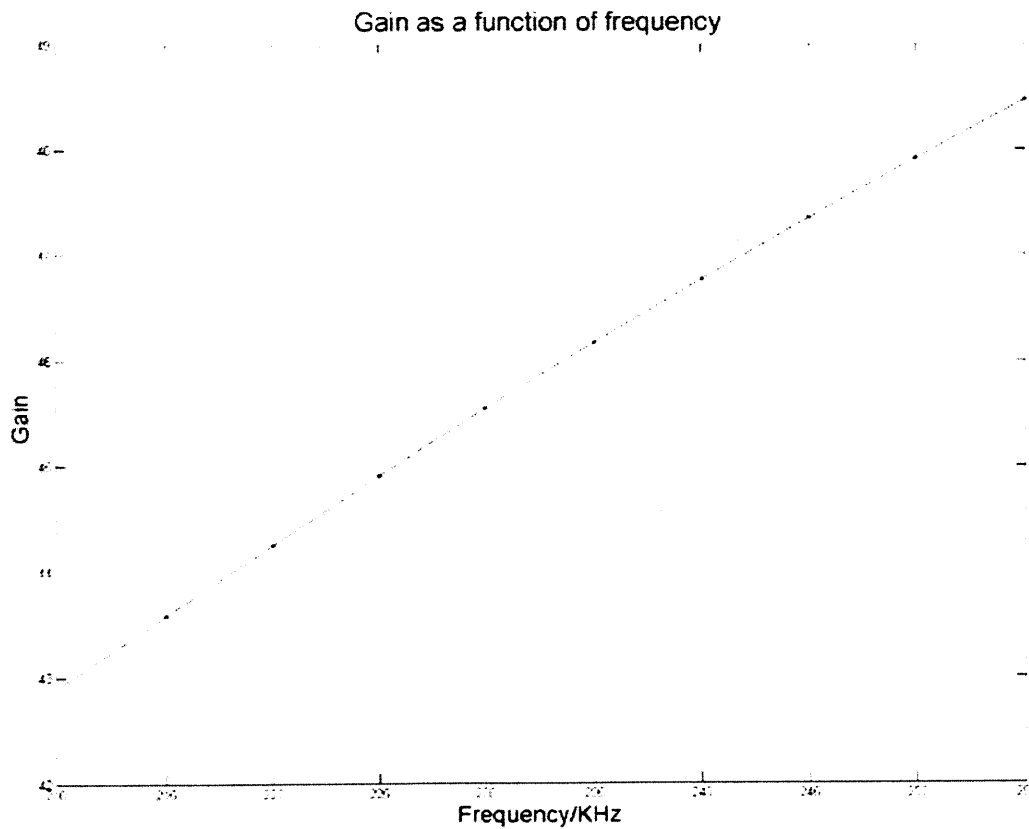


Figure 4 - 1 Gain as a Function of Frequency at stage I

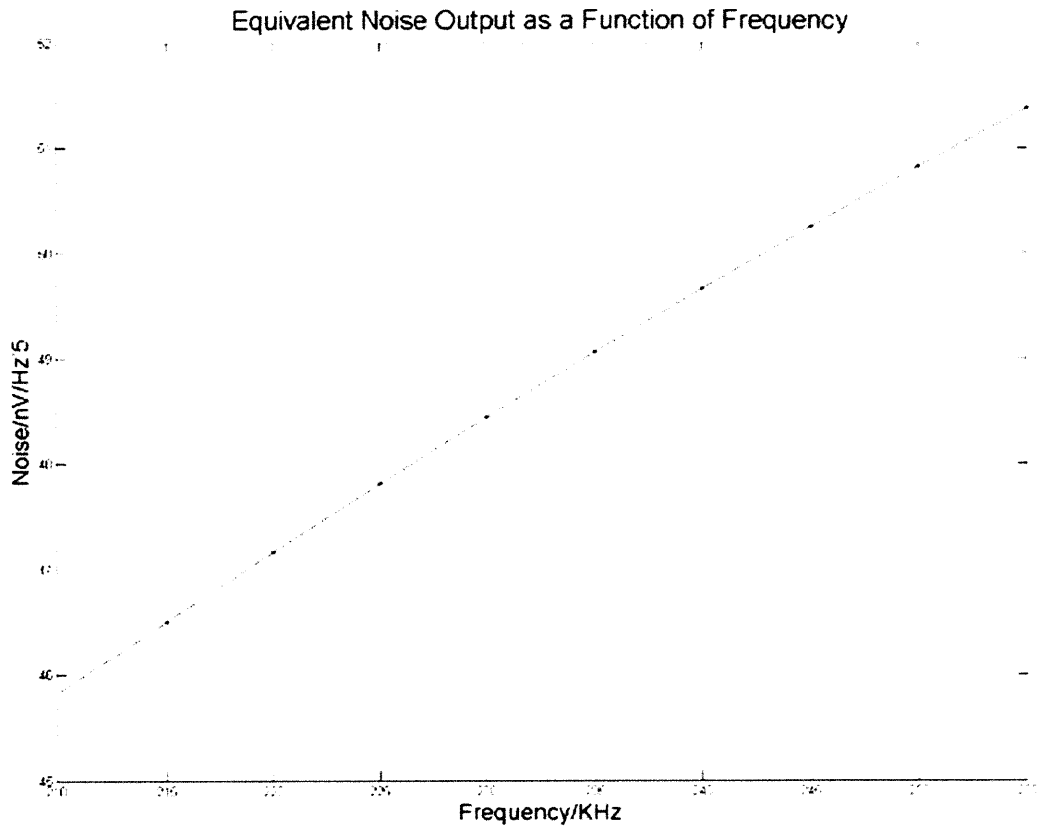


Figure 4 - 2 Simulated Antenna-Referenced Noise Voltage vs. Frequency at Stage I

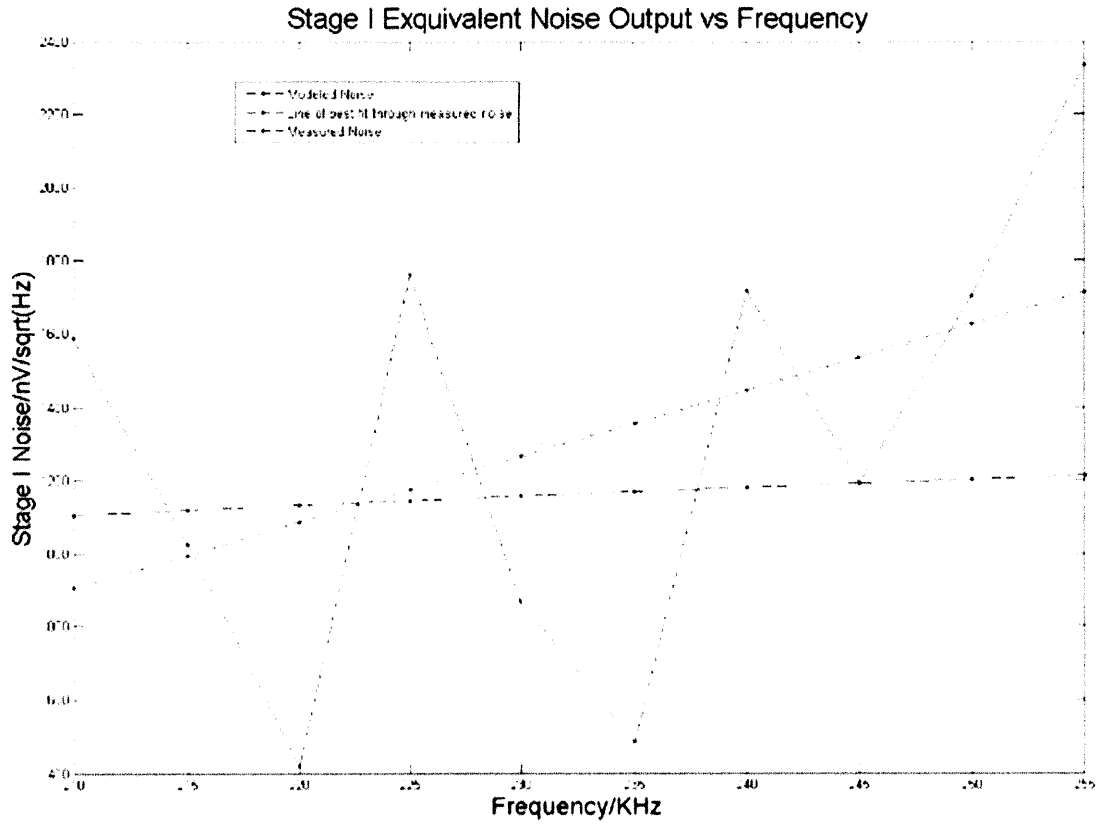


Figure 4 - 3 Measured Noise Voltage vs. Frequency at Stage I Compared with Predicted Noise Voltage.

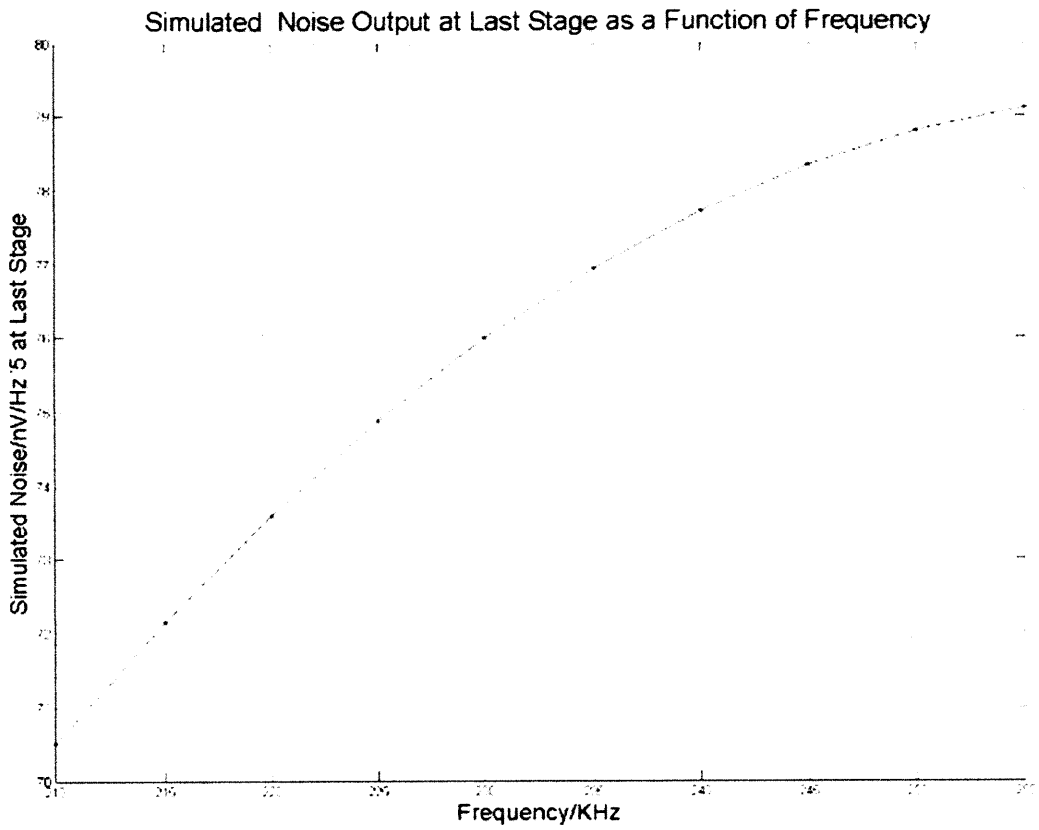


Figure 4 - 4 Antenna-Referenced SPICE Noise Voltage vs. frequency at Stage VII

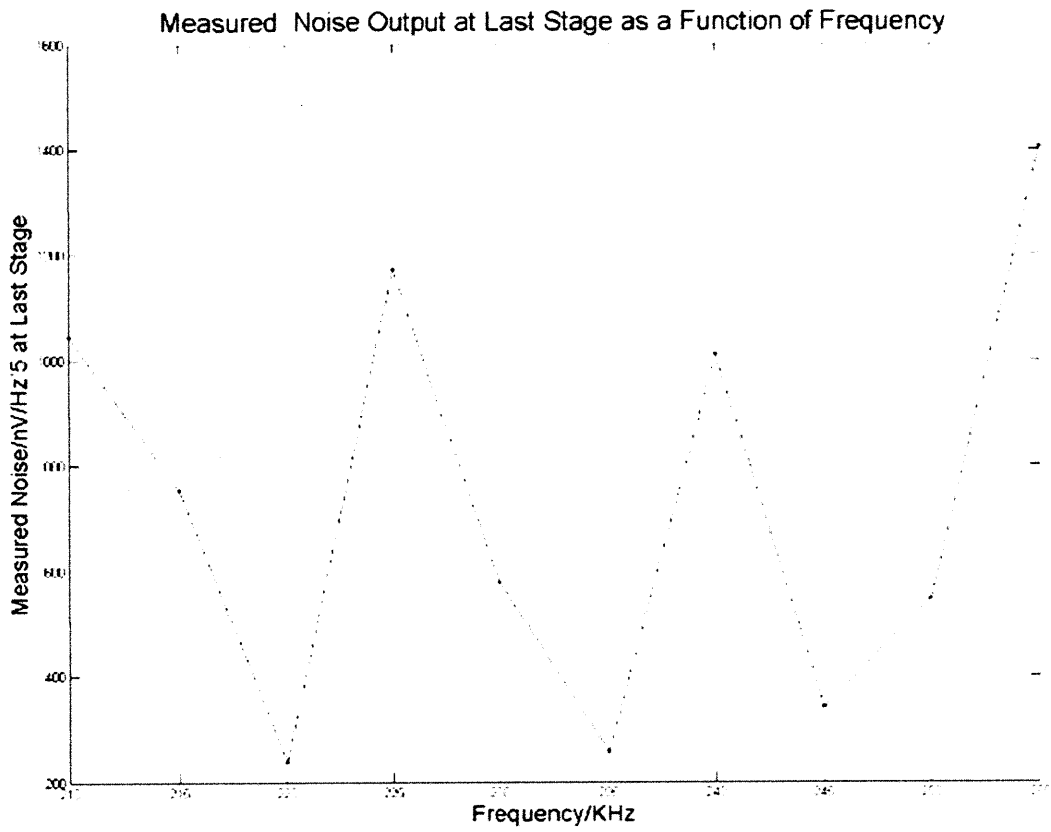


Figure 4 - 5 Measured Noise Voltage vs. Frequency at Stage 1 VII.

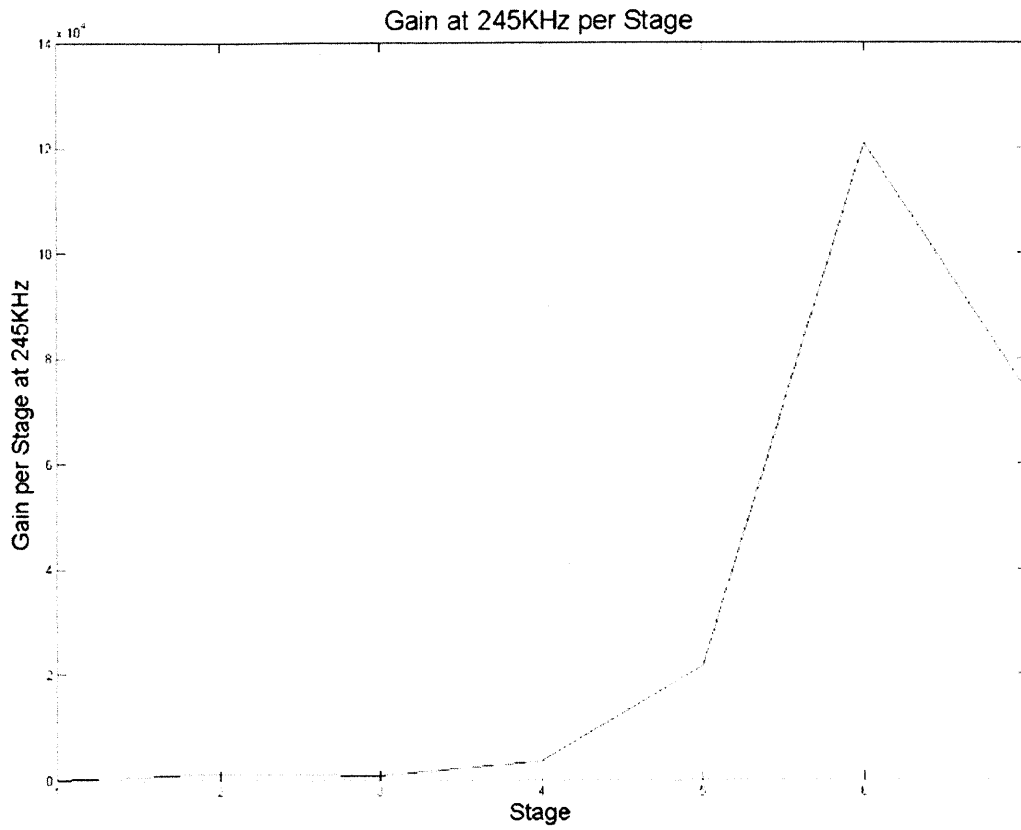


Figure 4 - 6 Simulated Gain at 245KHz for Stages 1 Through 7

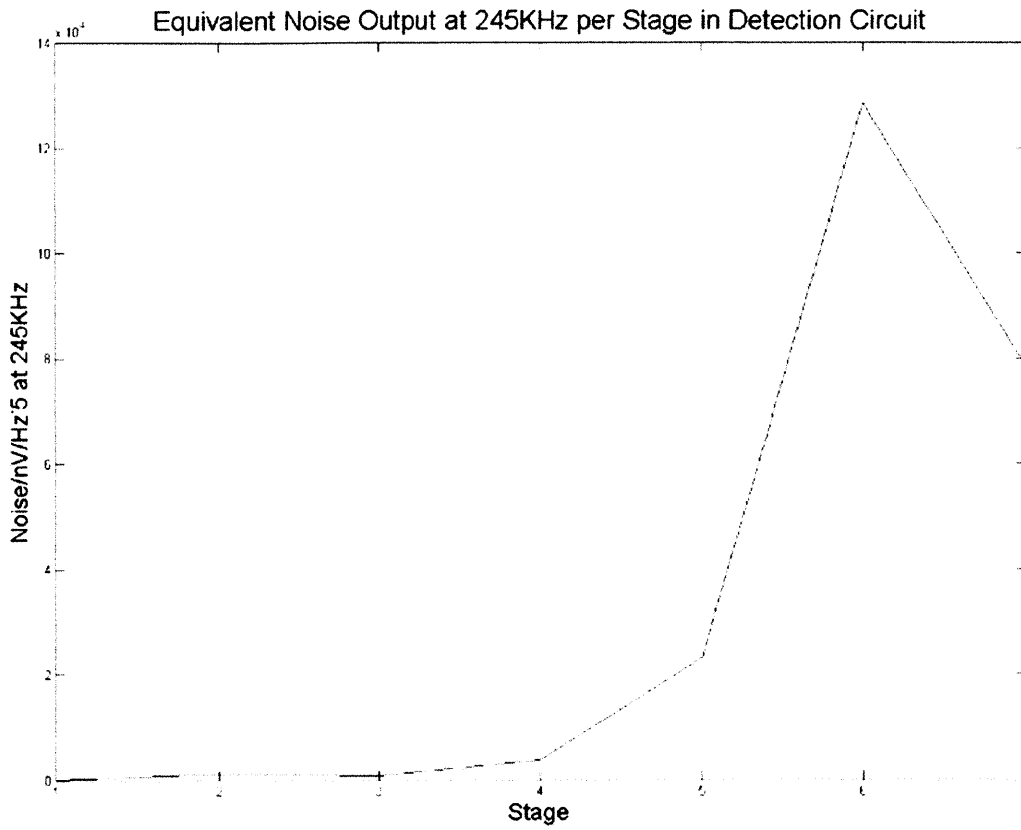


Figure 4 - 7 Simulated Antenna-Referenced Noise Voltage Input at 245KHz for Stages 1 Through 7

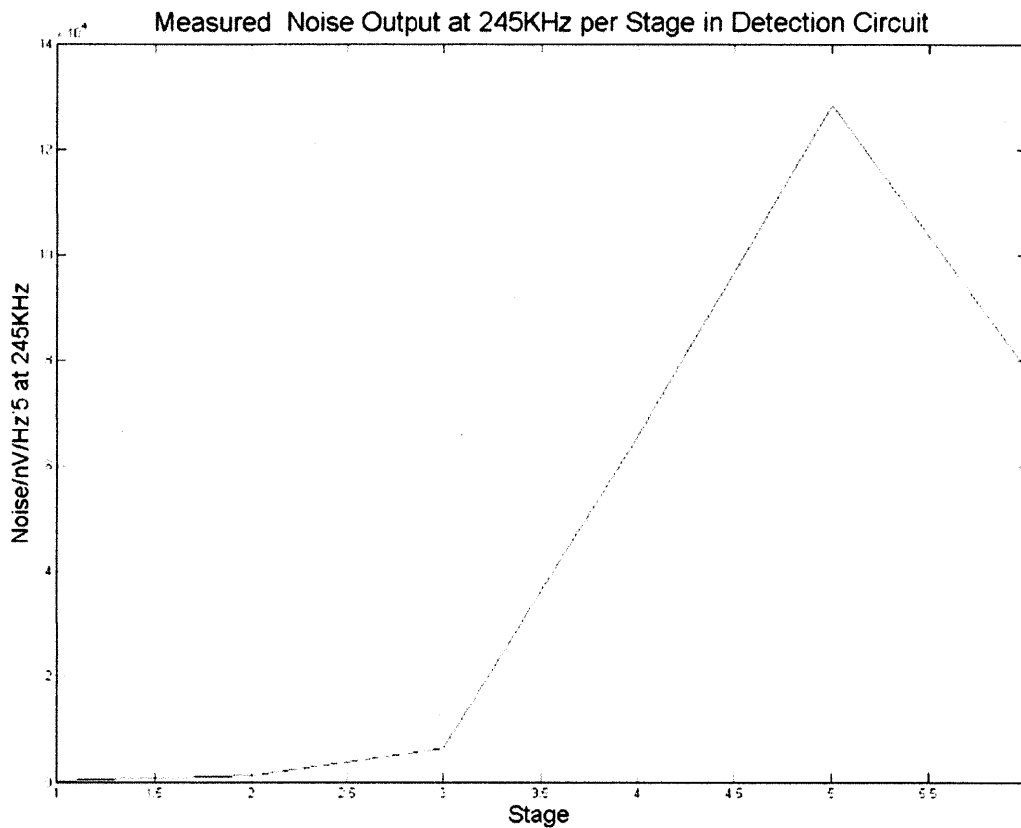


Figure 4 - 8 Measured Antenna-Referenced Noise Voltage Input at 245KHz for Stages 1 Through 6.

(The value at stage 4 could not be measured. Consequently any illustrated stage, I, beyond stage 3 is shown as stage i-1).

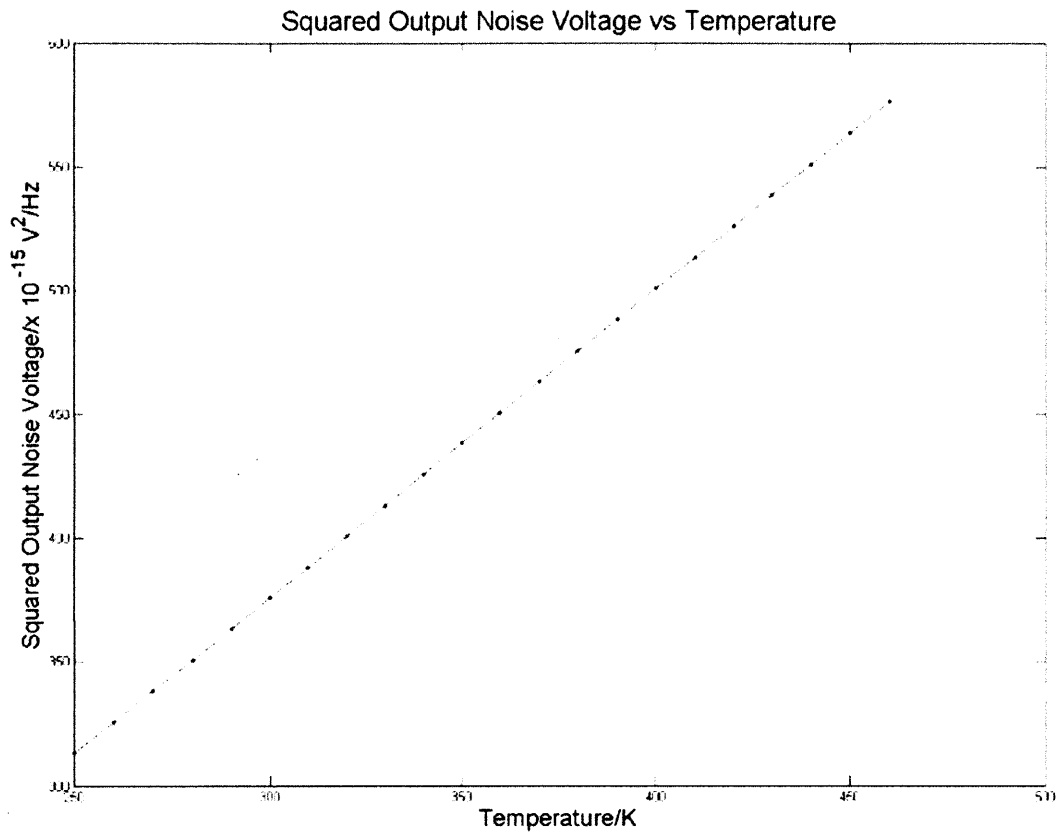


Figure 4 - 9 Simulated Noise Voltage vs. Temperature at Larmor Frequency

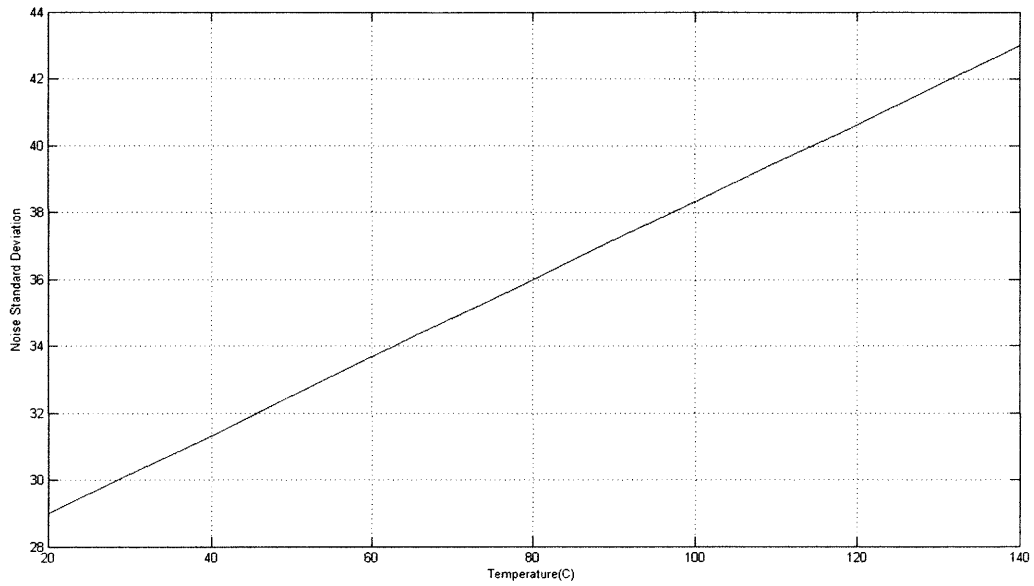


Figure 4 - 10 Measured Noise Voltage vs. Temperature at Larmor Frequency.

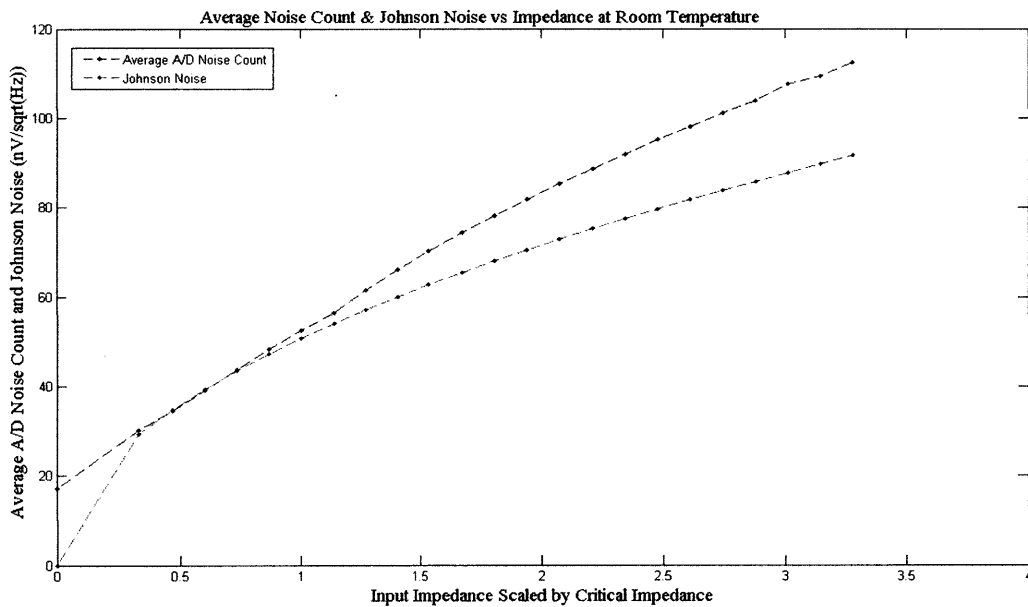


Figure 4 - 11 Simulated and Measured Noise Count vs. Input Impedance

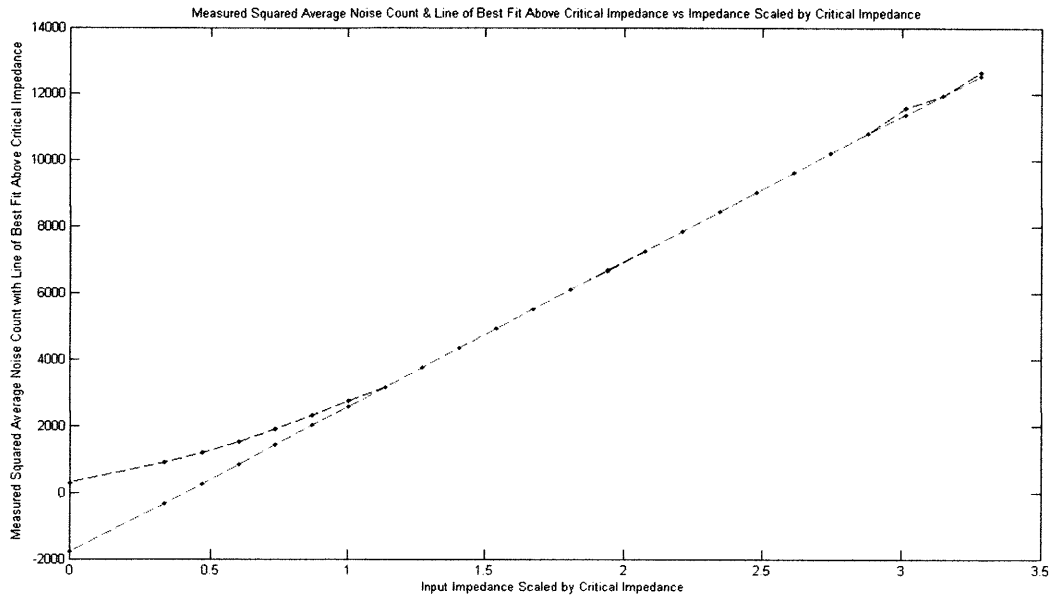


Figure 4 - 12 Measured Squared Average Noise Count vs. Input Impedance

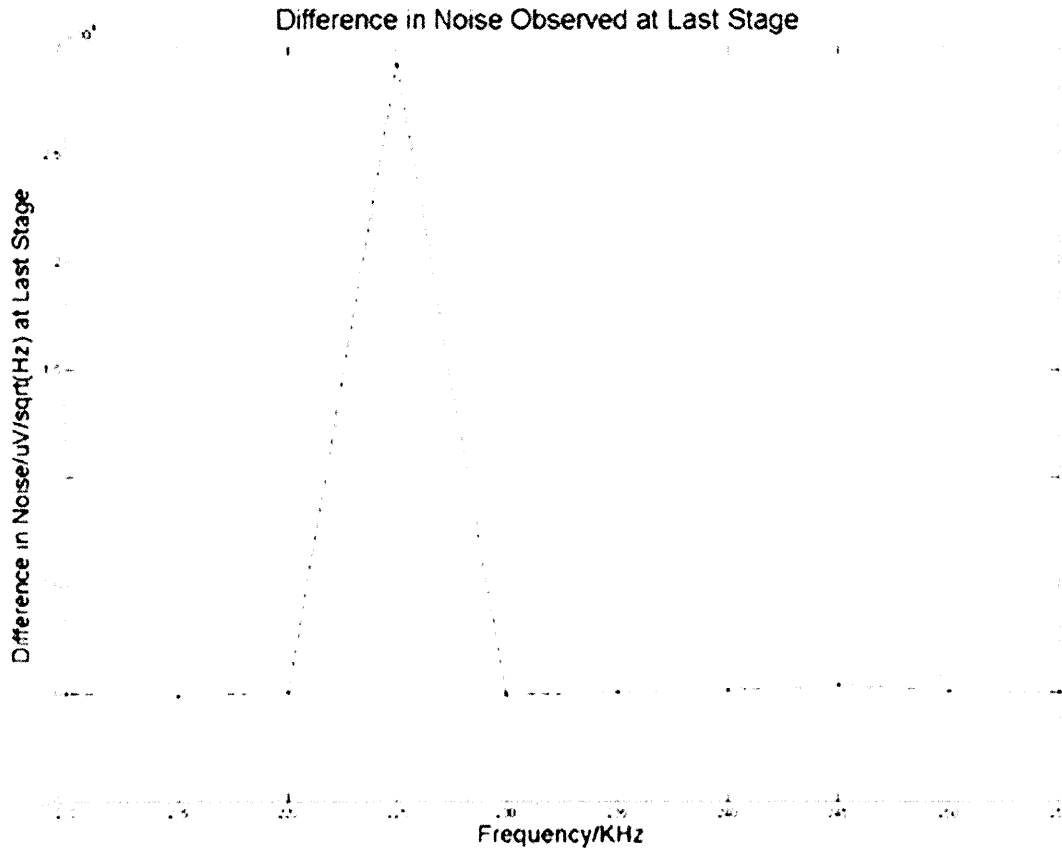


Figure 4 - 13 Difference in Measured Noise Voltage vs. Frequency at Stage 7 with Noise Source 1 On vs. Off

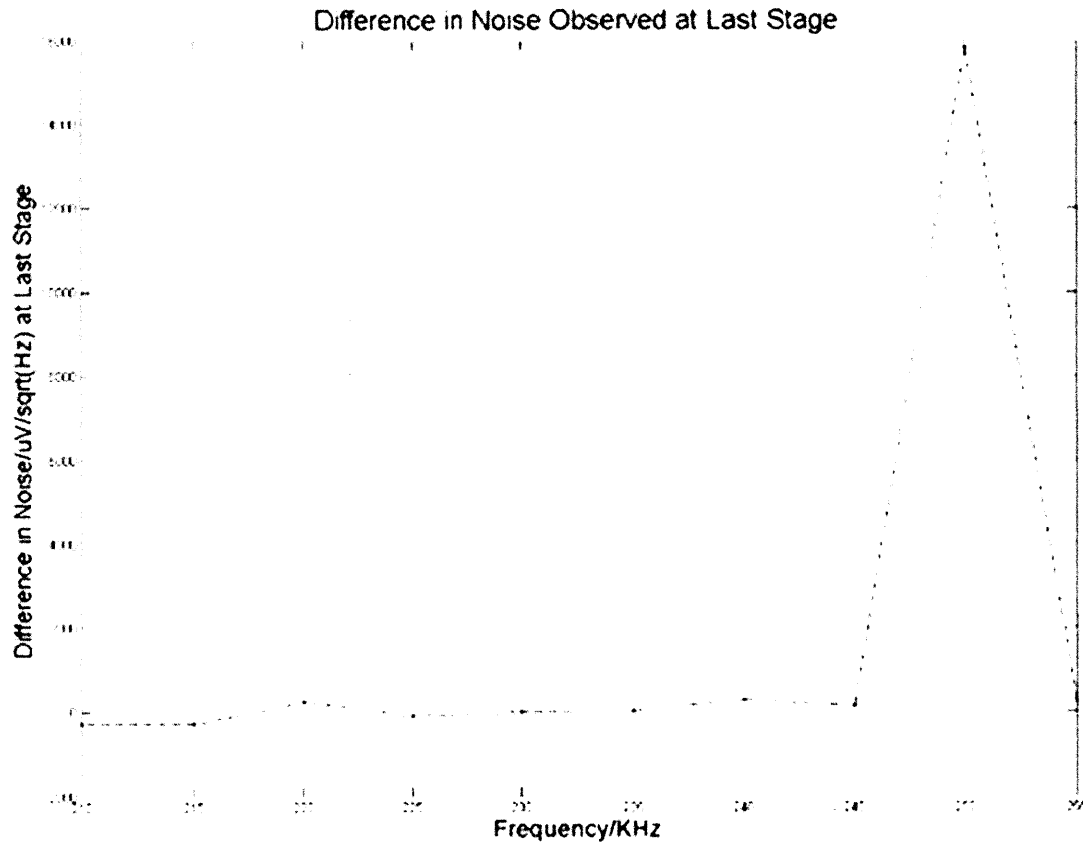


Figure 4 - 14 Difference in Measured Noise Voltage vs. Frequency at Stage 7 with Noise Source 2 On vs. Off

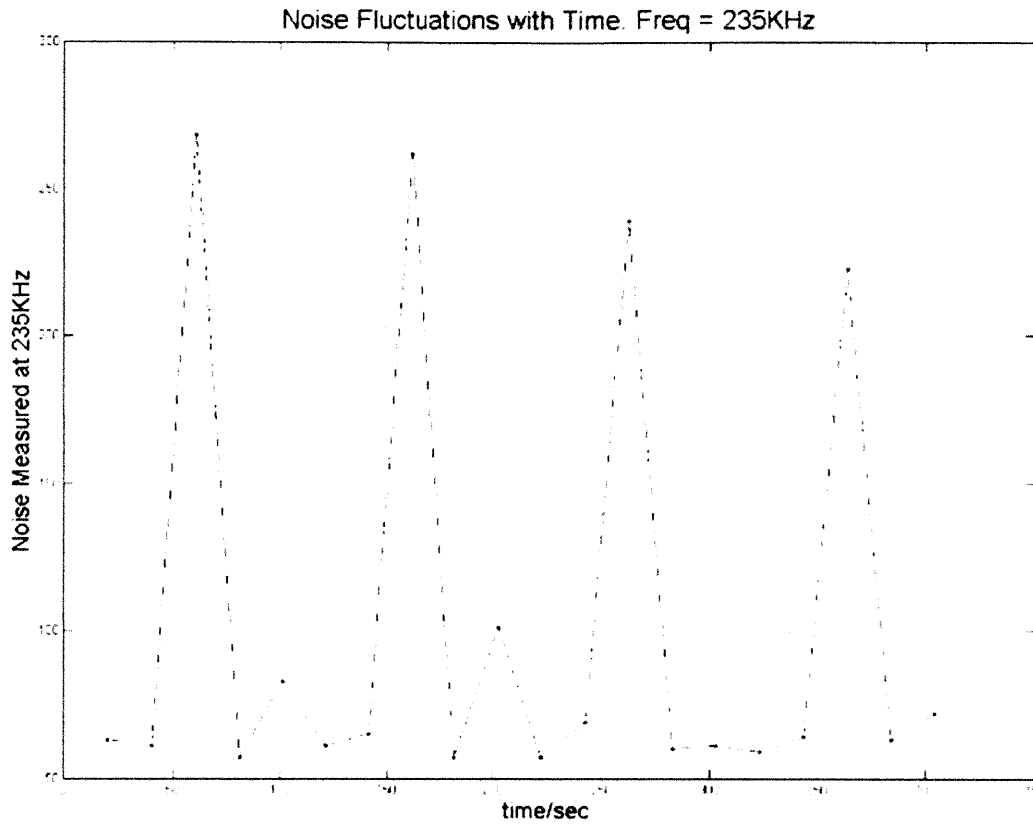


Figure 4 - 15 Transient Analysis of Noise Voltage at 235KHz

5. Discussion

It was expected that the noise voltage would be amplified by the same amounts as the signal with changes in frequency or across stages. The simulation results matched these expectations as visible in figure 4-2's noise voltage vs. frequency graph for stage I. The latter follows the same trend as the gain for the same stage in the previous figure. This pattern was observed in subsequent non-illustrated stages. Similarly, the noise per stage tracks the gain per stage (figures 4-7 and 4-6). This is reflected in the corresponding graphs per real noise, illustrating the conformity of the simulation with the real system.

Because the electrical noise in this system is dominated by Johnson noise, a linear variation of the square of the noise at the output of the detection circuitry was predicted by the simulation. Figure 4-10, the result of the confirmation experiment, also confirms this pattern

The predominance of Johnson noise also led to the prediction of a linear dependence of the squared noise output on the input impedance of the system. This was confirmed by the model and the experiments carried out on the tool. However, below the critical impedance, the squared noise flattened out (figure 4-12). A possible explanation for this is that normally the noise due to the input impedance of the first amplifier usually dominates the noise measured at the system output; it is the most amplified noise contribution in a system. If one keeps decreasing the input impedance of the first amplifier however, we are bound to reach a point beyond which the amplified value of the noise contributed by the impedance is no longer significant compared to the contribution of input impedances of amplifiers further along the noise path. Further decreases in input impedance at the first amplifier reduce the overall noise by smaller amounts until we hit the noise floor. In our case this "critical impedance" is the critical impedance previously mentioned and the noise floor is ~20 counts.

An unexpected result of the experiments on the tool was that transient measurement of the noise voltage showed periodic spikes in noise at 10KHz below the Larmor frequency and at the Larmor frequency as

per graph 4-15. The cause of this pattern could be interference from other circuitry or CPMG pulse side-effects. Figures 4-13 and 4-14 show, for example, that two potential coherent noise sources being on or off affects the noise measured two decades below the Larmor frequency.

One more measurement taken on the tool that deviated completely from expectation was the appearance of spikes in noise at unexpected frequencies as seen in figure 4-5. There are several possible explanations for these spikes, some of which could be remedied to by appropriate shielding. The first cause of the spikes could be interference from neighboring tools working at the spike frequencies. This noise agent would normally be a smaller nuisance if the experiments are run during non-business hours. Secondly the spikes could be occurring at harmonic or distortion frequencies of the frequency of interest.

5.1 Recommendations

The detection circuitry under analysis can be improved , as can be seen from the discussed deviations of the actual measurements from the noise model. For optimal functioning of the tool the agents causing these discrepancies need to be identified and attenuated. Some additional tests that could help with this endeavor are suggested below:

1. The tests should be rerun with the aid of an isolation transformer at the power input. This would help decouple the system from external circuits that could be contributing to noise.
2. While using the spectrum analyzer the use of a video bandwidth greater than the resolution bandwidth tends to help stabilize noise readings.
3. Two sources of electrical noise external to the detection circuitry were identified (see figures 4-14 and 4-15). These agents could be further investigated by, for example, using different types of circuitry that perform the same function and analyzing the setup under consideration for discrepancies in noise levels.

4. The noise vs. frequency tests should be run in a different lab other or with better timing reducing the effect of other tools' interference. This would help verify that the noise spikes at different frequencies are caused by neighboring equipment rather than the tool itself.
5. The LabVIEW code should be changed to plot noise vs. a continuous spectrum of values instead of noise at specific frequencies.

Modifications to the circuitry under inspection were proposed for future versions of the circuit boards to improve SNR. These suggestions were based on identified regions of signal gain improvement without noticeably altering Johnson noise.

5.2 Conclusion

SPICE provides a convenient modeling platform for electrical noise. The use of this software has helped create a model of the noise sources in the proVISION detection circuitry so as to determine the optimality of its performance. This has led to further research on the possible sources of disturbance responsible for deviations from the model and also gives users an immediate response idea of the consequences of SNR-improvement endeavors. It is consequently recommended that engineers always consider this approach in areas where SNR increase might benefit the functioning of a system of interest.

Appendix

A. Important Definitions

A.1 Noise Bandwidth, Δf

The noise bandwidth of a non-ideal system is the equivalent bandwidth of an ideal filter which passes the same amount of power as the non-ideal system, and has the same peak amplitude as this system. Hence:

$$\Delta f = \frac{1}{G_0} \int_0^\infty G(f) df \quad , \text{ or}$$

$$\Delta f = \frac{1}{A_{v0}^2} \int_0^\infty |A_v(f)|^2 df$$

Where G_0 = The peak amplitude of power gain,

$G(f)$ = power gain curve as a function of frequency,

A_{v0} = The peak amplitude of voltage gain curve,

$A_v(f)$ = The voltage gain curve as a function of frequency

A. 2 Nuclear Magnetic Resonance (NMR)

Nuclear Magnetic Resonance is a phenomenon exhibited by certain atoms in the presence of a static magnetic field and an electromagnetic pulse. Hydrogen atoms possess spins that lead them to behave like microscopic bar magnets. In the case of NMR these spins are primarily polarized

upon exposure to the strong static field, henceforth referred to as B_0 . The spins precess around the axis of this field until they are completely aligned with B_0 (ideally) at a frequency proportional to the field. They are then tipped into a plane transverse to their new equilibrium by an RF pulse, B_1 , after which they precess back to equilibrium with B_0 , emitting a detectable RF signal as they do so. In the oilfield industry, the atoms of interest are hydrogen which are abundant in oil and water, and are coincidentally the most sensitive atoms to NMR. The magnitude of the signal detected from the earth's formation is proportional to the number of Hydrogen atoms present. This fact, alongside relaxation times (the times taken to align or realign with B_0), is used to estimate rock porosity and pore-size distribution and identify fluids.

A.3 SPICE

SPICE or Simulated Program with Integrated Circuit Emphasis is a simulator used in design, verification and behavior prediction of analog electronic circuits. It is used to perform AC analysis, DC analysis, DC transfer curve analysis, Noise analysis, Transfer function analysis and Transient analysis mainly. This is done via either Netlists or Input Schematics with results viewable as Netlists and Plots.

B. Sample Calculation and Equivalent Simulation

The discussion below examines a basic non-inverting op-amp configuration, a standard section in many larger circuits.

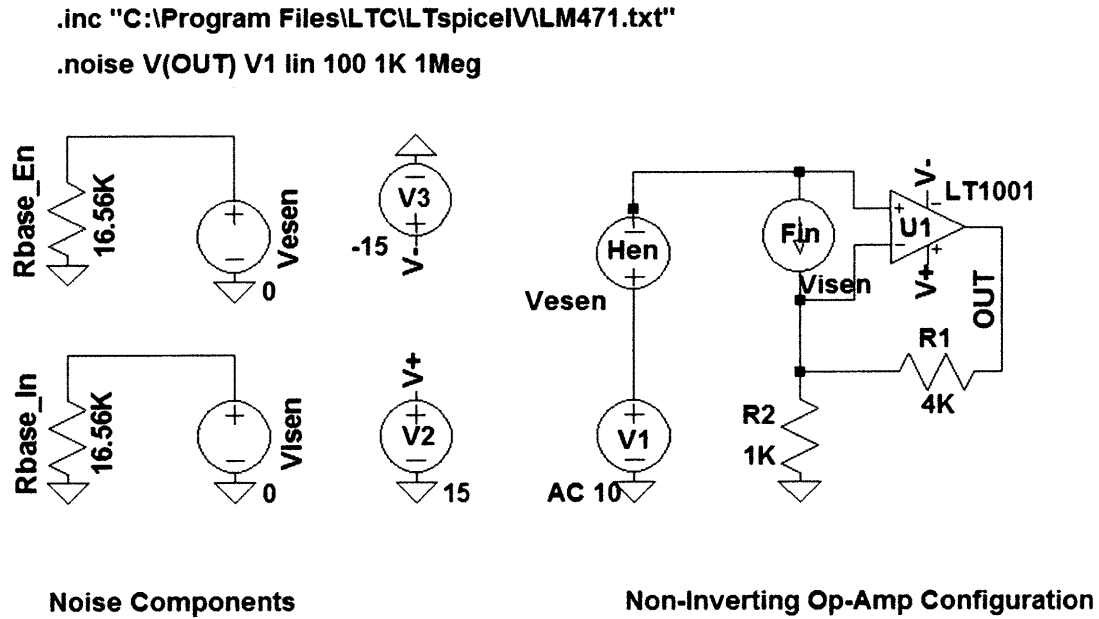


Fig B-1: Noisy circuit as described in SPICE simulation example.

B.2 Associated Netlist

```
* C:\Users\Julie\Desktop\Thesis\ThesisExampleAppendix.asc
Rbase_En N001 0 16.56K
Rbase_In N005 0 16.56K
Hen N006 N002 Vesen 4.5K
Fin N002 N004 Visen 0.01
Vesen N001 0 0
Visen N005 0 0
R1 N004 N003 4K
R2 0 N004 1K
V1 N006 0 AC 10
V2 V+ 0 15
V3 V- 0 -15
XU1 N002 N004 V+ V- N003 LT1001
.inc "C:\Program Files\LTC\LTspiceIV\LM471.txt"
```

```

.ac lin 1000 1K 500K
.lib LTC.lib
.backanno
.end

```

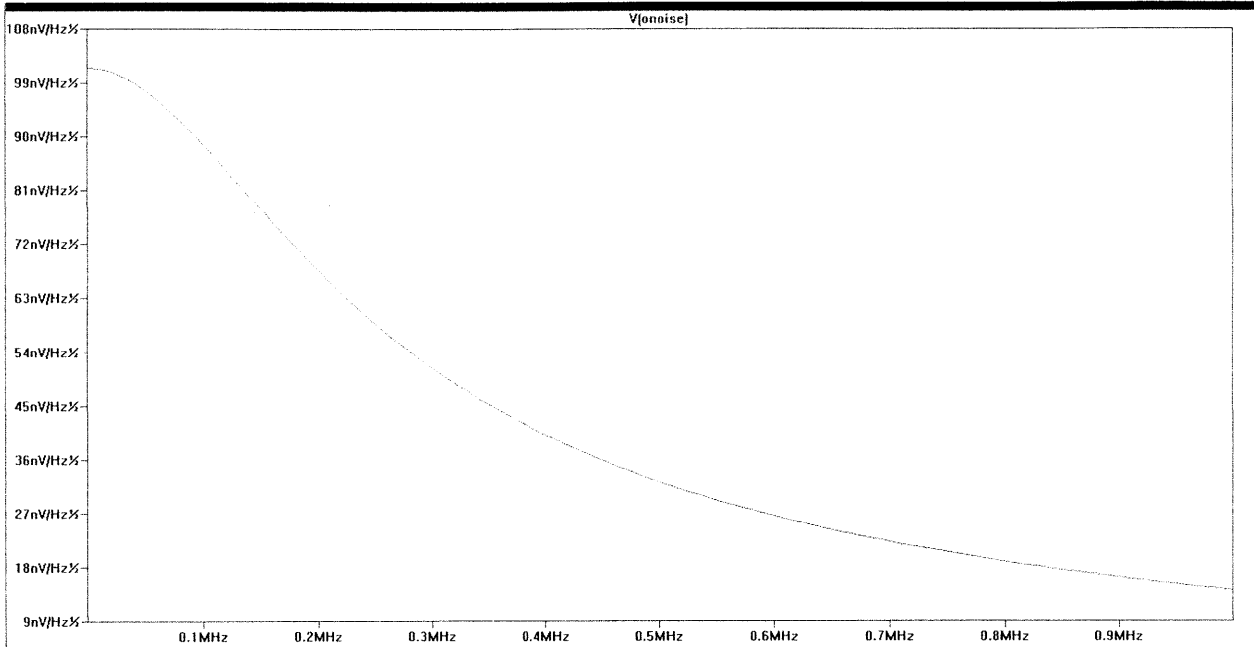


Fig B-2: Noise Plot of B-1 circuit

As per definition, the noise bandwidth Δf is the area under the power gain curve. In the case of the given simulation this value is $\sim 125\text{KHz}$. Calculating the noise at DC, according to our noise voltage equation,,

$$e_n = \sqrt{4K_B TR \Delta f}$$

We expect the calculated value to be approximately equal to 99nV at the output as per the graph. Assuming very no pass filtering given the amplifier used, the resistance seen at the output

$R = 5\Omega$, Hence,

$$e_n = \sqrt{4 \times 1.38 \times 10^{-23} \times 300 \times 5 \times 125 \times 10^3} = 101.2\text{nV}$$

This value be close enough to 99nV, keeping in mind that the noise bandwidth values is an approximation. These calculations can be repeated at several nodes of one's circuit to verify the model against theory.

C. References

Ballinger, Ray. "Introduction to MRI." MRITutor. Ed. Ray Ballinger. 12 Sep. 2009

<http://www.mritutor.org/mritutor/index.html>

De Jong, Marc. "Sub-Poissonian Shot Noise." Physics World Aug. 1996: 22

Howard, Roy M. Principles of Random Signal Analysis and Low Noise Design - The Power Spectral Density and its Application. New York: John Wiley & Sons, 2002.

KAIST Colossal Magento Resistance. 2009. 7 December 2009 <<http://mrm.kaist.ac.kr/cmr/>>

Motchenbacher, C.D. and Connelly, J.A. Low-Noise Electronic System Design New York: John Wiley & Sons, 1993

Personal discussions with Prof. Vladimir Stojanovic, Prof. Joel Dawson and Prof. Elfar Adalsteinsson

Personal discussions with Schlumberger Integration

Schlumberger. 2009. 7 December 2009 <<http://www.slb.com/>>